14th ITP/CAS–BLTP/JINR Joint Workshop
on Physics of Strong Interacting Systems
Oct. 18–23, 2026 Nanjing

Emergence of the nuclear halo in ^{22}C

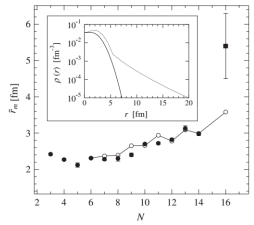
Bridging shape and shell

Xiang-Xiang Sun 孙向向
Institute of Theoretical Physics, Chinese Academy of Sciences
arXiv:2609.39753



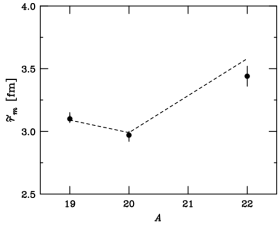
^{22}C: a Borromean halo, not yet pinned down

Halo nucleus: in a weakly bound system, valence nucleons occupy s- or p-wave orbits.



$R_m = 5.4 \pm 0.9$ fm (hydrogen target)

Tanaka et al., PRL **104**, 062701 (2010)



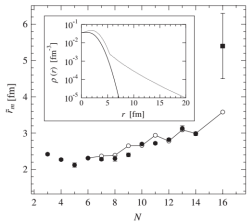
$R_m = 3.44 \pm 0.08$ fm (carbon target)

Togano et al., PLB **761**, 412 (2016)

- Breakup reaction: s-wave halo.
  Kobayashi et al., PRC **86**, 054604 (2012)

^{22}C: a Borromean halo, not yet pinned down

Halo nucleus: in a weakly bound system, valence nucleons occupy s- or p-wave orbits.

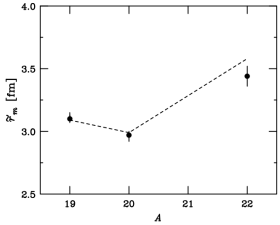


$R_m = 5.4 \pm 0.9$ fm (hydrogen target)

Tanaka et al., PRL **104**, 062701 (2010)

- Breakup reaction: s-wave halo.

  Kobayashi et al., PRC **86**, 054604 (2012)



$R_m = 3.44 \pm 0.08$ fm (carbon target)

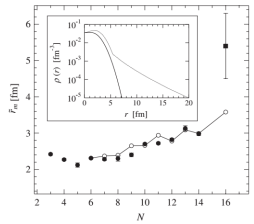
Togano et al., PLB **761**, 412 (2016)

- Glauber: $R_m = 3.38 \pm 0.10$ fm.

  Nagahisa et al., PRC **97**, 054614 (2018)

^{22}C: a Borromean halo, not yet pinned down

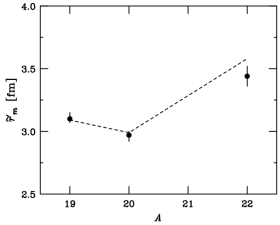
Halo nucleus: in a weakly bound system, valence nucleons occupy s- or p-wave orbits.



$R_m = 5.4 \pm 0.9$ fm (hydrogen target)

Tanaka et al., PRL **104**, 062701 (2010)

- Breakup reaction: s-wave halo.
  Kobayashi et al., PRC **86**, 054604 (2012)
- $S_{2n} = -0.14 \pm 0.46$ MeV (direct).
  Gaudefroy et al., PRL **109**, 202503 (2012)



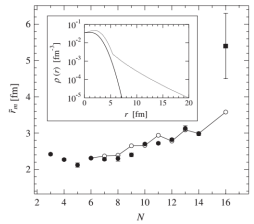
$R_m = 3.44 \pm 0.08$ fm (carbon target)

Togano et al., PLB **761**, 412 (2016)

- Glauber: $R_m = 3.38 \pm 0.10$ fm.
  Nagahisa et al., PRC **97**, 054614 (2018)
- $S_{2n} = 35 \pm 20$ keV (evaluated).
  Wang et al., Chin. Phys. C **45**, 030003 (2021)

^{22}C: a Borromean halo, not yet pinned down

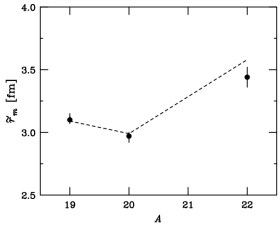
Halo nucleus: in a weakly bound system, valence nucleons occupy s- or p-wave orbits.



$R_m = 5.4 \pm 0.9$ fm (hydrogen target)

Tanaka et al., PRL **104**, 062701 (2010)

- Breakup reaction: s-wave halo.
  Kobayashi et al., PRC **86**, 054604 (2012)
- $S_{2n} = -0.14 \pm 0.46$ MeV (direct).
  Gaudefroy et al., PRL **109**, 202503 (2012)



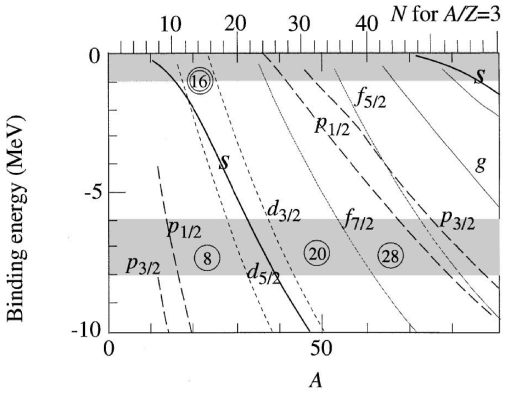
$R_m = 3.44 \pm 0.08$ fm (carbon target)

Togano et al., PLB **761**, 412 (2016)

- Glauber: $R_m = 3.38 \pm 0.10$ fm.
  Nagahisa et al., PRC **97**, 054614 (2018)
- $S_{2n} = 35 \pm 20$ keV (evaluated).
  Wang et al., Chin. Phys. C **45**, 030003 (2021)

The radius is still discrepant, and S_{2n} is poorly known.

Between collective ^{20}C and doubly magic ^{24}O



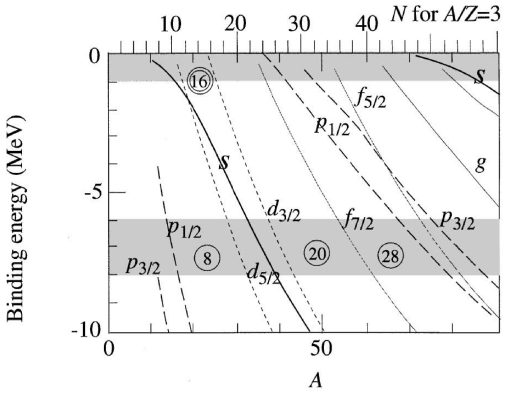
$N = 16$ emerges near the neutron drip line

Ozawa et al., PRL **84**, 5493 (2000)

- ^{24}O: $N = 16$ shell closure.
  $E(2^+) = 4.65 \pm 0.14$ MeV

  Tshoo et al., PRL **109**, 022501 (2012)

Between collective ^{20}C and doubly magic ^{24}O



$N = 16$ emerges near the neutron drip line

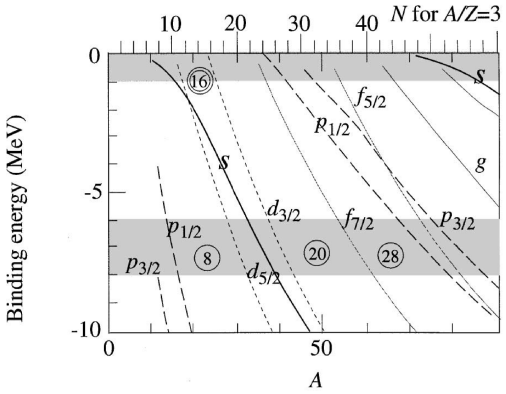
Ozawa et al., PRL **84**, 5493 (2000)

- ^{24}O: $N = 16$ shell closure.
  $E(2^+) = 4.65 \pm 0.14$ MeV

  Tshoo et al., PRL **109**, 022501 (2012)
- ^{20}C: $E(2^+) = 1.62$ MeV and
  $B(E2) = 7.5\ e^2\text{fm}^4$ indicates collectivity.

  Petri et al., PRL **107**, 102501 (2011)

Between collective ^{20}C and doubly magic ^{24}O



$N = 16$ emerges near the neutron drip line

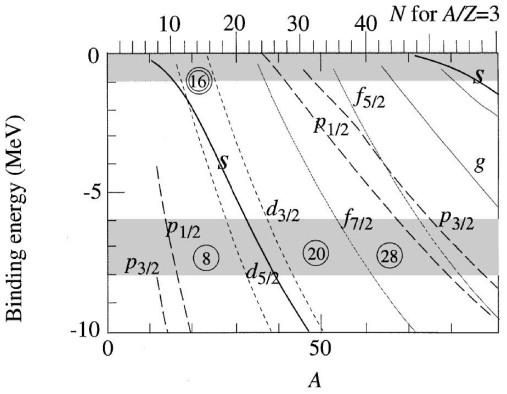
Ozawa et al., PRL **84**, 5493 (2000)

- ^{24}O: $N = 16$ shell closure.
  $E(2^+) = 4.65 \pm 0.14$ MeV

  Tshoo et al., PRL **109**, 022501 (2012)
- ^{20}C: $E(2^+) = 1.62$ MeV and
  $B(E2) = 7.5\ e^2\text{fm}^4$ indicates collectivity.

  Petri et al., PRL **107**, 102501 (2011)
- ^{22}C sits in between.

Between collective ^{20}C and doubly magic ^{24}O



$N = 16$ emerges near the neutron drip line

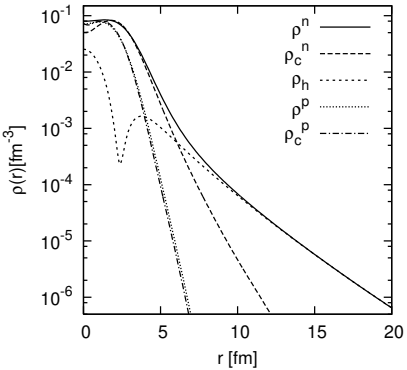
Ozawa et al., PRL **84**, 5493 (2000)

- ^{24}O: $N = 16$ shell closure.
  $E(2^+) = 4.65 \pm 0.14$ MeV
  Tshoo et al., PRL **109**, 022501 (2012)
- ^{20}C: $E(2^+) = 1.62$ MeV and
  $B(E2) = 7.5\ e^2\text{fm}^4$ indicates collectivity.
  Petri et al., PRL **107**, 102501 (2011)
- ^{22}C sits in between.

Inert s-wave halo, deformed like ^{20}C, or spherical $N = 16$?

Each existing picture captures one piece

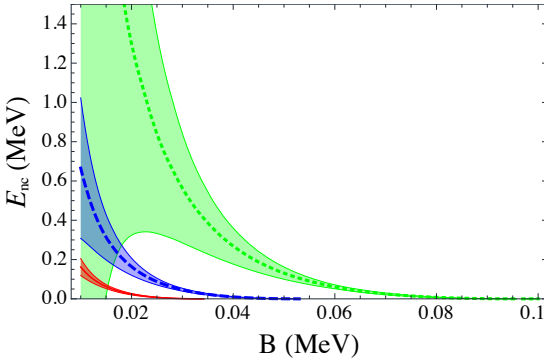
- Halo EFT and three-body model: ^{20}C–n scattering length
  Horiuchi & Suzuki, PRC **74**, 034311 (2006);
  Acharya et al., PLB **723**, 196 (2013)



^{20}C+$n+n$: halo density ρ_h, $(s_{1/2})^2$ dominant

Each existing picture captures one piece

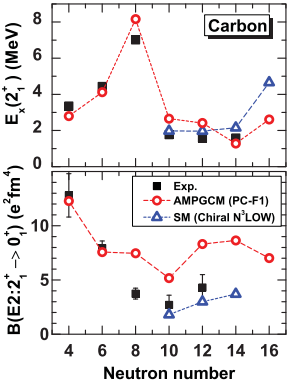
- Halo EFT and three-body model: ^{20}C–n scattering length
  Horiuchi & Suzuki, PRC **74**, 034311 (2006);
  Acharya et al., PLB **723**, 196 (2013)



Halo EFT: R_m contours in the plane of S_{2n} (B) and the ^{20}C–n virtual energy E_{nc}

Each existing picture captures one piece

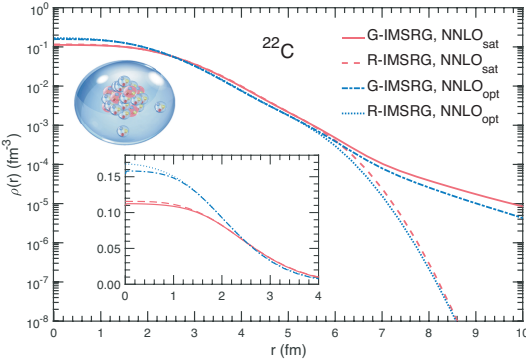
- Halo EFT and three-body model: ^{20}C–n scattering length
  Horiuchi & Suzuki, PRC **74**, 034311 (2006);
  Acharya et al., PLB **723**, 196 (2013)
- Shell model: $E(2^+) = 4.5$ MeV in ^{22}C.
  Coraggio et al., PRC **81**, 064303 (2010)
- AMP + GCM: samll $E(2^+)$ at $N = 16$.
  Yao et al., PRC **84**, 024306 (2011)



$J=0$ minimum $\beta = -0.40$. $E(2^+)$ stays low, $B(E2)$ stays finite. Oscillator basis, no continuum.

Each existing picture captures one piece

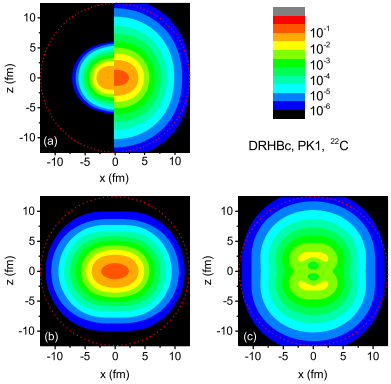
- Halo EFT and three-body model: ^{20}C–n scattering length
  Horiuchi & Suzuki, PRC **74**, 034311 (2006);
  Acharya et al., PLB **723**, 196 (2013)
- Shell model: $E(2^+) = 4.5$ MeV in ^{22}C.
  Coraggio et al., PRC **81**, 064303 (2010)
- AMP + GCM: samll $E(2^+)$ at $N = 16$.
  Yao et al., PRC **84**, 024306 (2011)
- Only *ab initio*: Gamow IMSRG.
  s-wave tail, no deformation.
  Hu et al., PRC **99**, 061302(R) (2019)



Gamow (G) vs real-energy (R) IMSRG:
the continuum s channel produces the tail

Each existing picture captures one piece

- Halo EFT and three-body model: ^{20}C–n scattering length
  Horiuchi & Suzuki, PRC **74**, 034311 (2006);
  Acharya et al., PLB **723**, 196 (2013)
- Shell model: $E(2^+) = 4.5$ MeV in ^{22}C.
  Coraggio et al., PRC **81**, 064303 (2010)
- AMP + GCM: samll $E(2^+)$ at $N = 16$.
  Yao et al., PRC **84**, 024306 (2011)
- Only *ab initio*: Gamow IMSRG.
  s-wave tail, no deformation.
  Hu et al., PRC **99**, 061302(R) (2019)
- DRHBc: deformed ground state has halo.
  Sun, Zhao & Zhou, PLB **785**, 530 (2018)

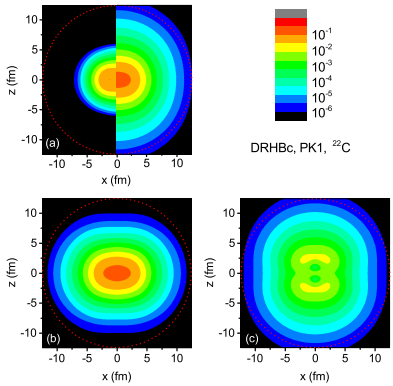


DRHBc (PK1): core, halo, and total densities.

Intrinsic frame only: $R_m = 3.25$ fm, no $B(E2)$.

Each existing picture captures one piece

- Halo EFT and three-body model: ^{20}C–n scattering length
  Horiuchi & Suzuki, PRC **74**, 034311 (2006);
  Acharya et al., PLB **723**, 196 (2013)
- Shell model: $E(2^+) = 4.5$ MeV in ^{22}C.
  Coraggio et al., PRC **81**, 064303 (2010)
- AMP + GCM: samll $E(2^+)$ at $N = 16$.
  Yao et al., PRC **84**, 024306 (2011)
- Only *ab initio*: Gamow IMSRG.
  s-wave tail, no deformation.
  Hu et al., PRC **99**, 061302(R) (2019)
- DRHBc: deformed ground state has halo.
  Sun, Zhao & Zhou, PLB **785**, 530 (2018)



DRHBc (PK1): core, halo, and total densities.

Intrinsic frame only: $R_m = 3.25$ fm, no $B(E2)$.

No model yet treats deformation, continuum, and spectroscopy.

From DRHBc to MR-DRHBc

- DRHBc: Deformed Relativistic Hartree–Bogoliubov theory in continuum.
  Deformation and the continuum. Only for intrinsic frame, no collective excitations.
  Zhou et al., PRC **82**, 011301(R) (2010); Li et al., PRC **85**, 024312 (2012)

From DRHBc to MR-DRHBc

- DRHBc: Deformed Relativistic Hartree–Bogoliubov theory in continuum.
  Deformation and the continuum. Only for intrinsic frame, no collective excitations.
  Zhou et al., PRC **82**, 011301(R) (2010); Li et al., PRC **85**, 024312 (2012)
- MR-DRHBc: Multi-Reference DFT based on DRHBc.
  PNP, AMP, and configuration mixing on DRHBc states $|\Phi(\beta)\rangle$.
  Sun & Zhou, Sci. Bull. **66**, 1521 (2021); PRC **104**, 064319 (2021)
  Sun, arXiv:2609.39753

$$|\Psi_\alpha^{JNZ}\rangle = \sum_\beta f_\alpha^{JNZ}(\beta)\ \hat{P}^J \hat{P}^N \hat{P}^Z\, |\Phi(\beta)\rangle$$

Hill–Wheeler equation

$$\sum_{\beta'} \Big[\mathcal{H}(\beta,\beta') - E_\alpha \mathcal{N}(\beta,\beta')\Big] f_\alpha^{JNZ}(\beta') = 0$$

Collective wave function: $g_\alpha^{JNZ} = \mathcal{N}^{1/2} f_\alpha^{JNZ}$

From DRHBc to MR-DRHBc

- DRHBc: Deformed Relativistic Hartree–Bogoliubov theory in continuum.
  Deformation and the continuum. Only for intrinsic frame, no collective excitations.
  Zhou et al., PRC **82**, 011301(R) (2010); Li et al., PRC **85**, 024312 (2012)
- MR-DRHBc: Multi-Reference DFT based on DRHBc.
  PNP, AMP, and configuration mixing on DRHBc states $|\Phi(\beta)\rangle$.
  Sun & Zhou, Sci. Bull. **66**, 1521 (2021); PRC **104**, 064319 (2021)
  Sun, arXiv:2609.39753

$$|\Psi_\alpha^{JNZ}\rangle = \sum_\beta f_\alpha^{JNZ}(\beta)\ \hat{P}^J \hat{P}^N \hat{P}^Z\, |\Phi(\beta)\rangle$$

Hill–Wheeler equation

$$\sum_{\beta'} \Big[\mathcal{H}(\beta,\beta') - E_\alpha\, \mathcal{N}(\beta,\beta')\Big] f_\alpha^{JNZ}(\beta') = 0$$

Collective wave function: $g_\alpha^{JNZ} = \mathcal{N}^{1/2} f_\alpha^{JNZ}$

- Three point-coupling functionals: PC-F1, PC-PK1, DD-PC1.

From DRHBc to MR-DRHBc

- DRHBc: Deformed Relativistic Hartree–Bogoliubov theory in continuum.
  Deformation and the continuum. Only for intrinsic frame, no collective excitations.
  Zhou et al., PRC **82**, 011301(R) (2010); Li et al., PRC **85**, 024312 (2012)
- MR-DRHBc: Multi-Reference DFT based on DRHBc.
  PNP, AMP, and configuration mixing on DRHBc states $|\Phi(\beta)\rangle$.
  Sun & Zhou, Sci. Bull. **66**, 1521 (2021); PRC **104**, 064319 (2021)
  Sun, arXiv:2609.39753

$$|\Psi_\alpha^{JNZ}\rangle = \sum_\beta f_\alpha^{JNZ}(\beta)\ \hat{P}^J \hat{P}^N \hat{P}^Z\, |\Phi(\beta)\rangle$$

Hill–Wheeler equation

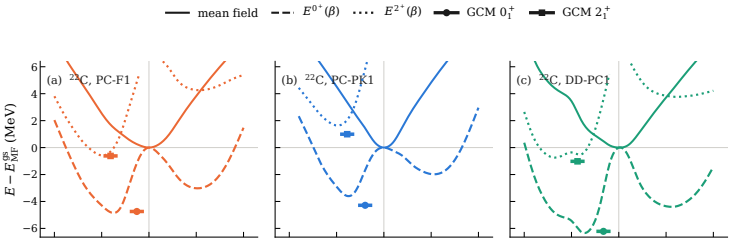
$$\sum_{\beta'} \Big[\mathcal{H}(\beta,\beta') - E_\alpha \mathcal{N}(\beta,\beta')\Big] f_\alpha^{JNZ}(\beta') = 0$$

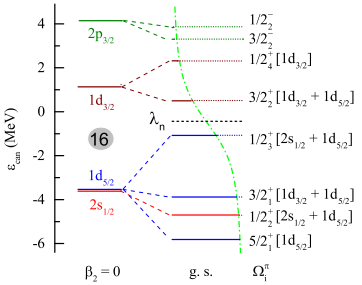
Collective wave function: $g_\alpha^{JNZ} = \mathcal{N}^{1/2} f_\alpha^{JNZ}$

- Three point-coupling functionals: PC-F1, PC-PK1, DD-PC1.

The framework is universal for exotic nuclei.

The halo appears beyond the mean field



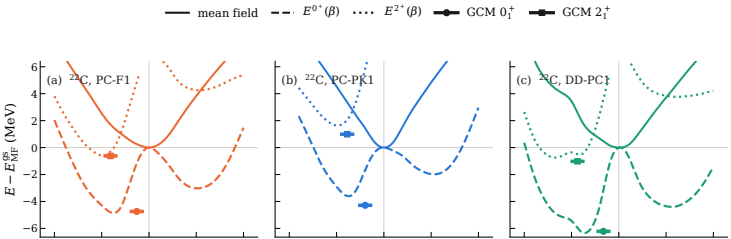


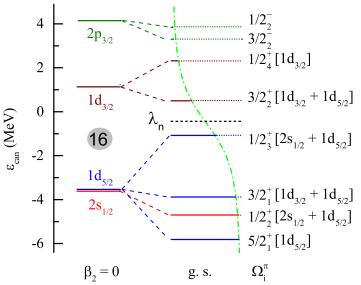
- Mean field: spherical & no halo ($R_m = 3.12$–3.17 fm).

PK1: spherical limit and ground state.

Sun, Zhao & Zhou, PLB **785**, 530 (2018)

The halo appears beyond the mean field



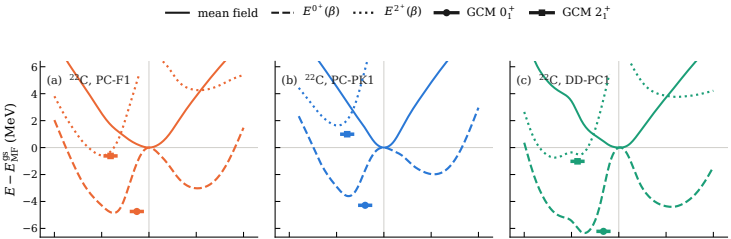


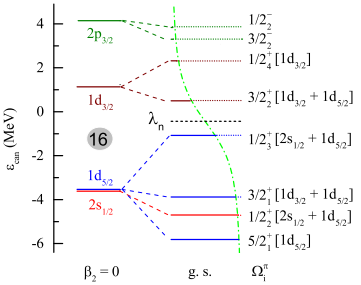
- Mean field: spherical & no halo ($R_m = 3.12$–3.17 fm).
- $J = 0$: minimum at $\beta \approx -0.4$.

PK1: spherical limit and ground state.

Sun, Zhao & Zhou, PLB **785**, 530 (2018)

The halo appears beyond the mean field



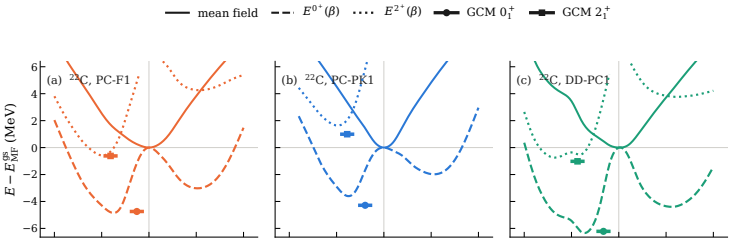


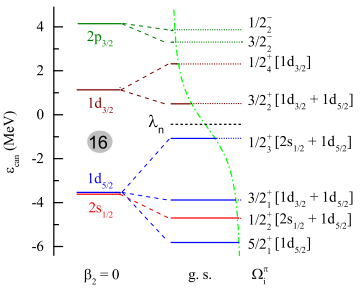
- Mean field: spherical & no halo ($R_m = 3.12$–3.17 fm).
- $J = 0$: minimum at $\beta \approx -0.4$.
- Mixing: $R_m \approx 3.29$ fm, all three functionals.

PK1: spherical limit and ground state.

Sun, Zhao & Zhou, PLB **785**, 530 (2018)

The halo appears beyond the mean field





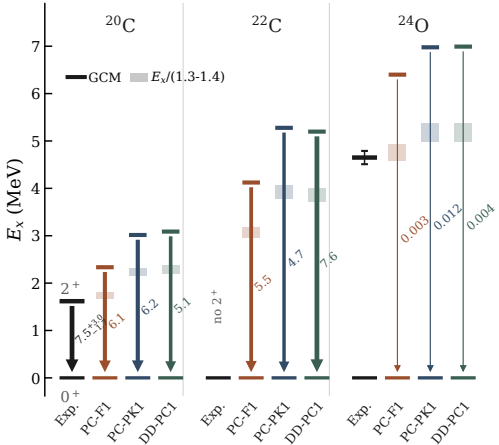
- Mean field: spherical & no halo ($R_m = 3.12$–3.17 fm).
- $J = 0$: minimum at $\beta \approx -0.4$.
- Mixing: $R_m \approx 3.29$ fm, all three functionals.

PK1: spherical limit and ground state.

Sun, Zhao & Zhou, PLB **785**, 530 (2018)

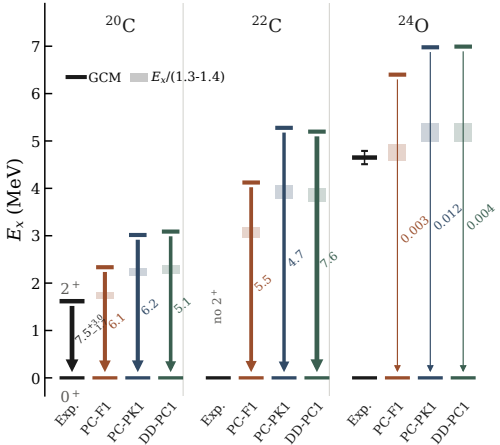
Without projection, ^{22}C has no halo with point-coupling functionals.

$B(E2)$ follows ^{20}C, not ^{24}O



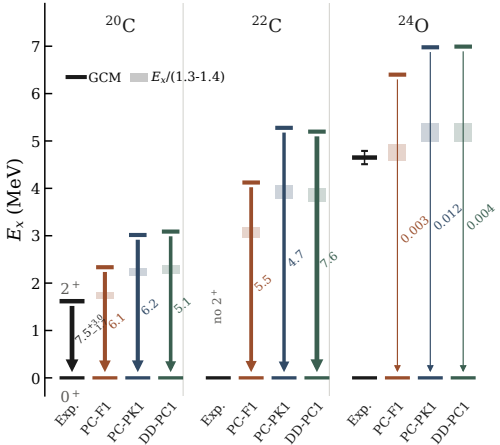
- $B(E2; 2^+ \to 0^+)$ in $e^2\text{fm}^4$:
  - ^{24}O ≈ 0
  - ^{20}C 5–6 (exp. 7.5)
  - ^{22}C 4.7–7.6

$B(E2)$ follows ^{20}C, not ^{24}O



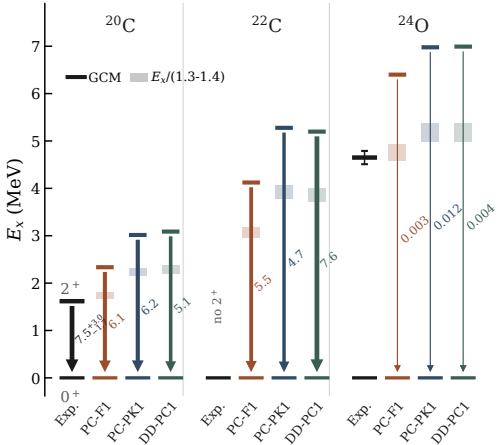
- $B(E2; 2^+ \to 0^+)$ in $e^2\text{fm}^4$:
  ^{24}O ≈ 0
  ^{20}C 5–6 (exp. 7.5)
  ^{22}C 4.7–7.6
- $E(2^+) \approx 1.7\times$ that of ^{20}C.

$B(E2)$ follows ^{20}C, not ^{24}O



- $B(E2; 2^+ \to 0^+)$ in $e^2\text{fm}^4$:
  ^{24}O ≈ 0
  ^{20}C 5–6 (exp. 7.5)
  ^{22}C 4.7–7.6
- $E(2^+) \approx 1.7\times$ that of ^{20}C.
- AMP overestimates E_x; ratios and $B(E2)$ are robust.

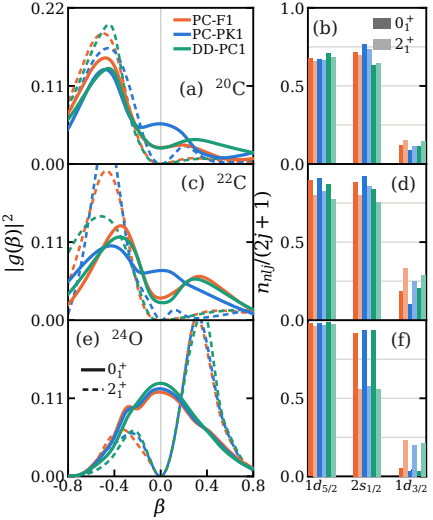
$B(E2)$ follows ^{20}C, not ^{24}O



- $B(E2; 2^+ \to 0^+)$ in $e^2\text{fm}^4$:
  ^{24}O ≈ 0
  ^{20}C 5–6 (exp. 7.5)
  ^{22}C 4.7–7.6
- $E(2^+) \approx 1.7\times$ that of ^{20}C.
- AMP overestimates E_x; ratios and $B(E2)$ are robust.

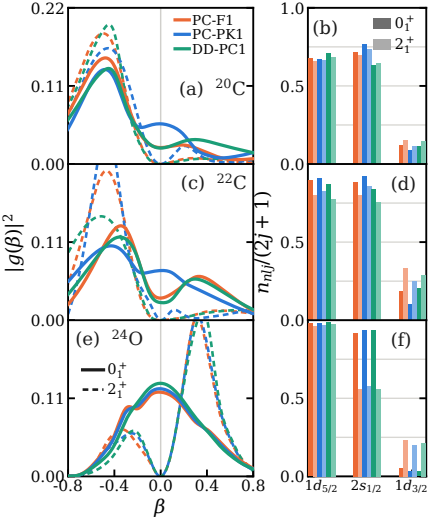
^{22}C is a collective rotor like ^{20}C.

Oblate and soft; $N = 16$ is weakened



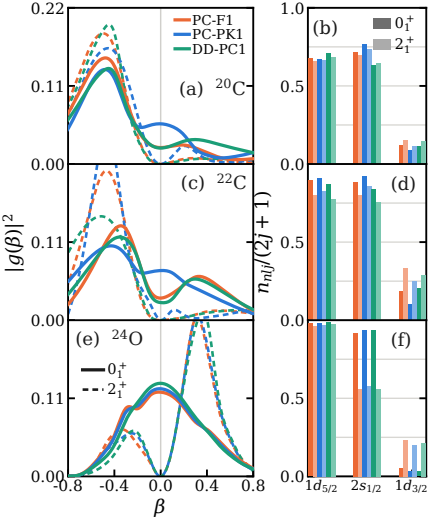
- ^{20,22}C peak near $\beta \approx -0.4$; ^{24}O stays at $\beta = 0$.

Oblate and soft; $N = 16$ is weakened



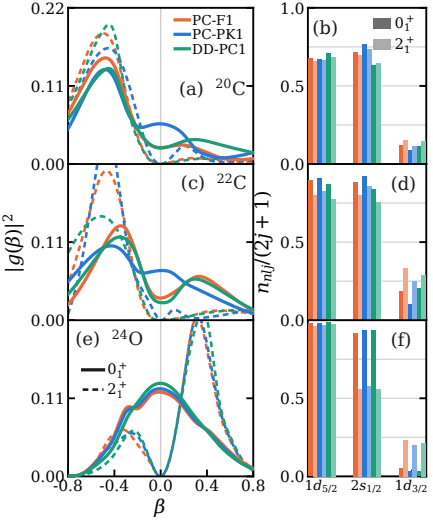
- ^{20,22}C peak near $\beta \approx -0.4$; ^{24}O stays at $\beta = 0$.
- ^{22}C is soft: shape mixing; $\langle\beta\rangle = -0.13$ to -0.20.

Oblate and soft; $N = 16$ is weakened



- ^{20,22}C peak near $\beta \approx -0.4$; ^{24}O stays at $\beta = 0$.
- ^{22}C is soft: shape mixing; $\langle\beta\rangle = -0.13$ to -0.20.
- 2^+ of ^{24}O: particle–hole excitation. 2^+ of ^{22}C: mostly rotational.

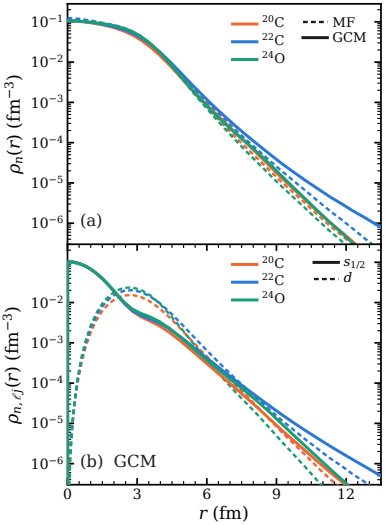
Oblate and soft; $N = 16$ is weakened



- ^{20,22}C peak near $\beta \approx -0.4$; ^{24}O stays at $\beta = 0$.
- ^{22}C is soft: shape mixing; $\langle\beta\rangle = -0.13$ to -0.20.
- 2^+ of ^{24}O: particle–hole excitation. 2^+ of ^{22}C: mostly rotational.

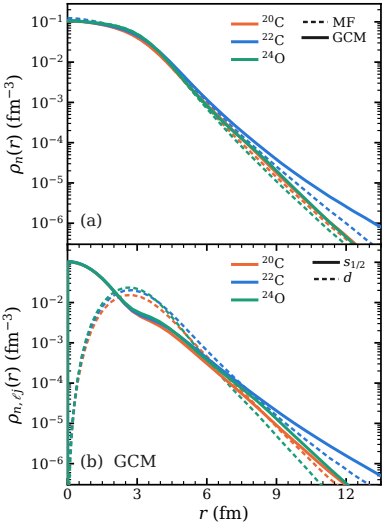
About 0.4 neutrons cross $N = 16$ into $1d_{3/2}$ in ^{22}C.

An s-wave tail on an sd mixture



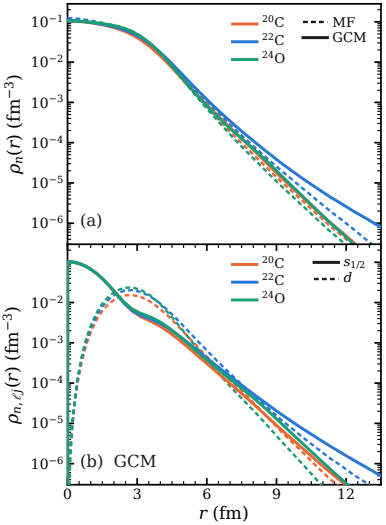
- Mean field: No obvious tail.

An s-wave tail on an sd mixture



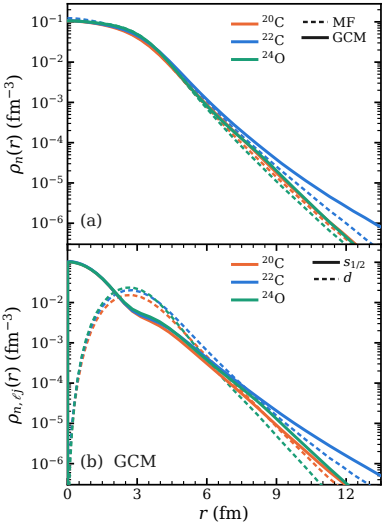
- Mean field: No obvious tail.
- With shape mixing: Tail appears.

An s-wave tail on an sd mixture



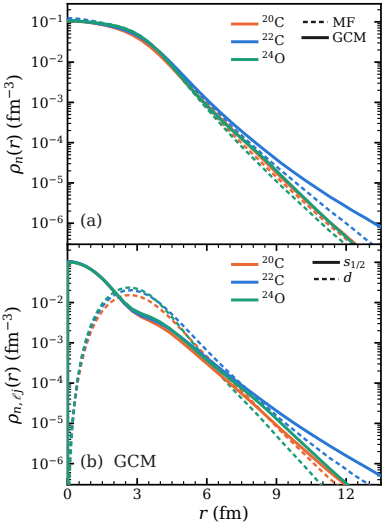
- Mean field: No obvious tail.
- With shape mixing: Tail appears.
- d waves match $s_{1/2}$ out to ~ 8 fm; beyond that, $s_{1/2}$ dominates.

An s-wave tail on an sd mixture



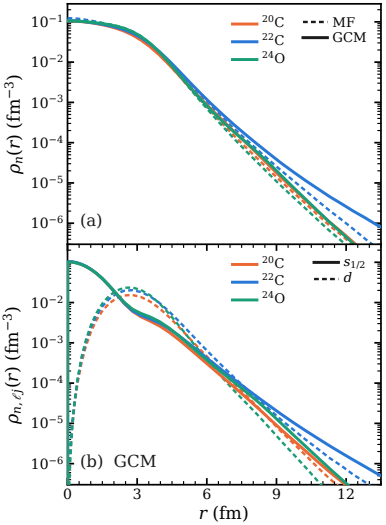
- Mean field: No obvious tail.
- With shape mixing: Tail appears.
- d waves match $s_{1/2}$ out to ~ 8 fm; beyond that, $s_{1/2}$ dominates.
- $R_m = 3.29$ fm.

An s-wave tail on an sd mixture



- Mean field: No obvious tail.
- With shape mixing: Tail appears.
- d waves match $s_{1/2}$ out to ~ 8 fm; beyond that, $s_{1/2}$ dominates.
- $R_m = 3.29$ fm.
- PC-F1 shown; PC-PK1 and DD-PC1 agree.

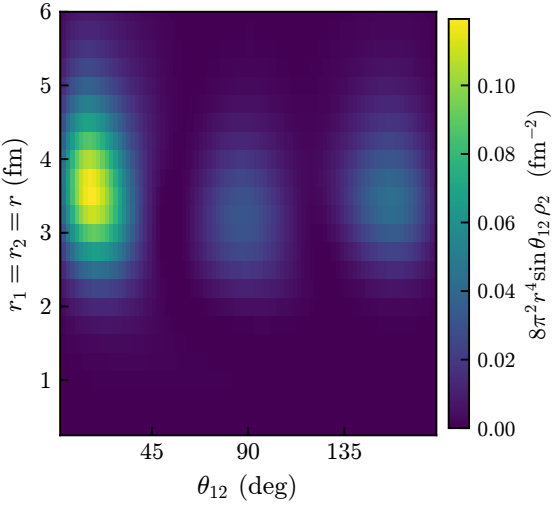
An s-wave tail on an sd mixture



- Mean field: No obvious tail.
- With shape mixing: Tail appears.
- d waves match $s_{1/2}$ out to ~ 8 fm; beyond that, $s_{1/2}$ dominates.
- $R_m = 3.29$ fm.
- PC-F1 shown; PC-PK1 and DD-PC1 agree.

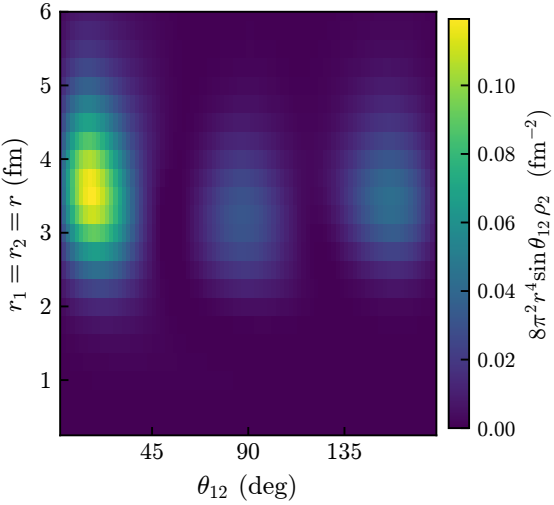
$R_m = 3.29$ fm, next to 3.38 ± 0.10 fm (Glauber).

The valence neutrons form a dineutron



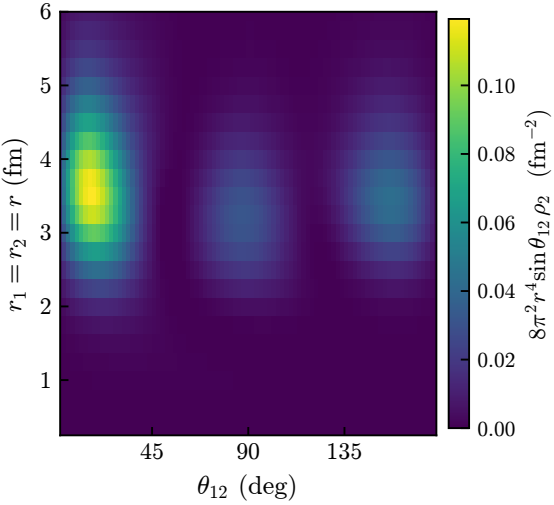
- $J^\pi = 0^+$ state at $\beta = -0.4$ (PC-F1).

The valence neutrons form a dineutron



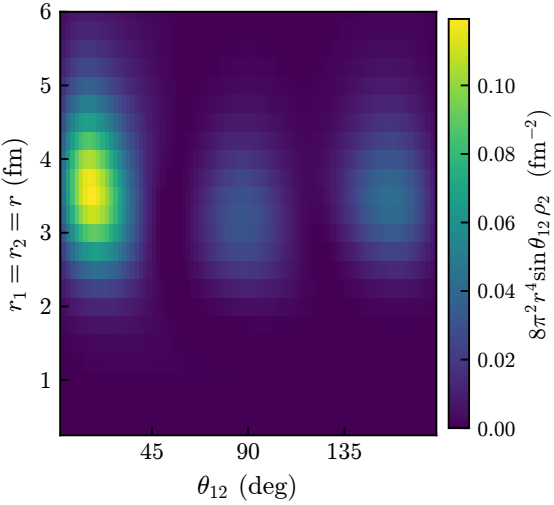
- $J^\pi = 0^+$ state at $\beta = -0.4$ (PC-F1).
- Peak at $r \approx 3.5$ fm, $\theta_{12} \approx 18^\circ$.

The valence neutrons form a dineutron



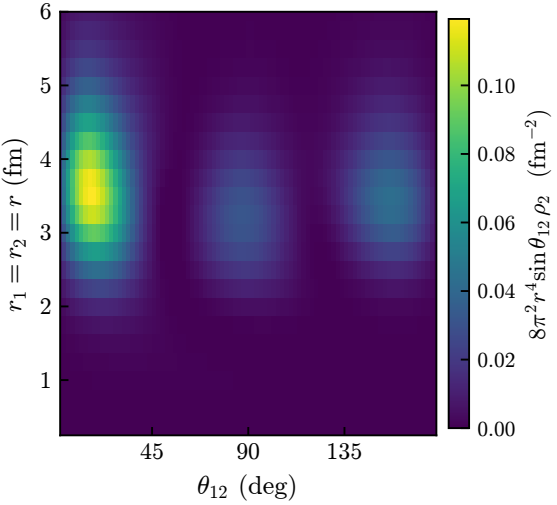
- $J^\pi = 0^+$ state at $\beta = -0.4$ (PC-F1).
- Peak at $r \approx 3.5$ fm, $\theta_{12} \approx 18°$.
- 59% of the pair at $\theta_{12} < 60°$.

The valence neutrons form a dineutron

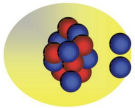


- $J^\pi = 0^+$ state at $\beta = -0.4$ (PC-F1).
- Peak at $r \approx 3.5$ fm, $\theta_{12} \approx 18^\circ$.
- 59% of the pair at $\theta_{12} < 60^\circ$.
- Cluster sum rule: $B(E1) \sim 1.5\ e^2\text{fm}^2$ (integrated).

The valence neutrons form a dineutron



- $J^\pi = 0^+$ state at $\beta = -0.4$ (PC-F1).
- Peak at $r \approx 3.5$ fm, $\theta_{12} \approx 18°$.
- 59% of the pair at $\theta_{12} < 60°$.
- Cluster sum rule: $B(E1) \sim 1.5\ e^2\text{fm}^2$ (integrated).



A compact dineutron on an oblate core.

Summary

- **Method:** MR-DRHBc keeps the continuum and deformation, restores J and particle number, and mixes shapes.
- **Mechanism:** Beyond mean field effects are important to halo.
- **Halo:** ^{22}C is a deformed two-neutron halo, $R_m = 3.29$ fm, s-wave tail on an sd mixture, dineutron pair.
- **Shell:** $B(E2)$ follows ^{20}C; $N = 16$ is weakened, not restored.
- **Robust:** three point-coupling functionals agree; meson-exchange DRHBc also gives a deformed halo.
- **Outlook:** odd-A (deformed) halo nuclei: ^{29,31}F, ^{31}Ne, ^{37}Mg.

Thank you!

Backup: GCM yrast states

		$E_x(2^+)$	$B(E2)$	R_m	$\langle\beta\rangle$	S_{2n}
^{20}C	exp.	1.62	7.5			
^{20}C	PC-F1	2.34	6.11	3.15	-0.39	
^{20}C	PC-PK1	3.02	6.23	3.12	-0.25	
^{20}C	DD-PC1	3.09	5.09	3.11	-0.29	
^{22}C	PC-F1	4.12	5.51	3.29	-0.13	$+0.86$
^{22}C	PC-PK1	5.28	4.74	3.29	-0.20	$+0.56$
^{22}C	DD-PC1	5.20	7.58	3.29	-0.16	-0.56
^{24}O	PC-F1	6.40	0.003	3.12	$+0.04$	
^{24}O	PC-PK1	6.98	0.012	3.13	$+0.04$	
^{24}O	DD-PC1	6.92	0.039	3.10	$+0.02$	

Units: MeV, e^2fm^4, fm. Mean field of ^{22}C is spherical, $R_m = 3.12$–3.17 fm.